



Original Article

Effect of inlet throttling on thermohydraulic instability in a large scale water-based RCCS: A system-level analysis with RELAP5-3D

Zhilee Jhia Ooi^{*}, Qiuping Lv, Rui Hu, Matthew Jasica, Darius Lisowski

Argonne National Laboratory, 9700 S. Cass Ave., Lemont, 60439, IL, USA



ARTICLE INFO

Keywords:

System-level modeling
RELAP5-3D
RCCS
Safety analysis
NSTF

ABSTRACT

This paper presents results from system-level modeling of a water-based reactor cavity cooling system using RELAP5-3D. The computational model is benchmarked with experimental data from a half-scale RCCS test facility at Argonne National Laboratory. The model prediction is first compared with a two-phase oscillatory baseline experimental case where mixed accuracy is obtained. The model shows reasonable prediction of mass flow rate, pressure, and temperature but significant overprediction of void fraction. The model prediction is then compared with a fault case where the inlet of the risers is gradually reduced using a throttling valve. As the valve is closed, the model is able to predict some major flow phenomena observed in the experiment such as the dampening of oscillations, the reintroduction of oscillations, as well as boiling, flashing, and geysering in the risers. However, the timeline of these events are not well captured by the model. The model is also used to investigate the evolution of flow regime in the chimney. This work highlights that the semi-empirical constitutive relations used in RELAP-3D could have a strong influence on the accuracy of the model in two-phase oscillatory flows.

1. Introduction

The High Temperature Reactor (HTR) is one of the candidates for the Gen-IV reactor designs that are currently under development. The HTRs appeal to the nuclear industry due to their inherent safety features, high thermal-to-electric conversion efficiency, and the ability to provide high-temperature process heat [1]. Many HTR designs rely on the Reactor Cavity Cooling System (RCCS) for passive decay heat removal and safe reactor shutdown during accident scenarios due to its relatively simple design, the reliance on natural forces, and the potential for high levels of performance [2]. The RCCS is designed to ensure that the vessel wall and the fuel peak temperatures are maintained at safe limits during normal operation and accident scenarios, to maintain the reactor cavity concrete and support structures at safe limits, to sustain the intended function and performance across the 40-year life span of a reactor installation, and to accomplish the above functions without human intervention or active systems [2].

Different designs of RCCS have been explored, among them the water-cooled RCCS design. The water in the RCCS is designed to maintain at low temperature and atmospheric pressure during normal operation. However, during certain accident scenarios where the cooling capability of the primary coolant flow is compromised, the RCCS is designed to operate in two-phase conditions as it undergoes phase change phenomena. Given the no active systems nor human

intervention design philosophy of the RCCS, the flow of coolant in the system is driven entirely by natural circulation. This means that a long chimney section is often required in RCCS to provide sufficient thermal driving head to ensure that the natural circulation in the system reaches the desired flow rate to effectively remove decay heat from the reactor. However, at the same time, the requirement exposes the system to two-phase instabilities and flow oscillations especially when flashing occurs in the chimney. These oscillations could severely reduce the heat removal capability of the RCCS and potentially compromise the structural integrity of the system. Given the severe consequences of the failure of the system during accident scenarios, it is paramount to understand the thermal hydraulics behavior of the RCCS in order to ensure that the system can operate as designed.

As an effort to improve the current understanding of the RCCS, a program was established at Argonne National Laboratory (Argonne) under the support of the United States Department of Energy (US-DOE) Office of Advanced Reactor Technologies (ART) to develop technologies to improve the reliability and safety of new reactor designs [2]. Under the program, an experimental test assembly known as the Natural convection Shutdown heat removal Test Facility (NSTF) was constructed at Argonne to investigate the feasibility of the RCCS. To achieve this goal the NSTF has continuously produced NQA-1 compliant experimental

^{*} Corresponding author.

E-mail address: zooi@anl.gov (Z.J. Ooi).

data that could be utilized for supporting licensing of safety features in advanced reactor designs since early 2014. The experimental data are used for validating and verifying safety related codes that in turn are used by vendors and regulatory bodies to assess the feasibility and limits of these safety features such as the RCCS. Given the increased reliance on safety analysis codes for the determination of safety margins, course of accident progression, design of new reactor concepts and systems, and regulatory justification, it is critical to ensure that these codes and computational tools can correctly predict the behaviors of nuclear reactors and safety features especially during accident scenarios.

Many current RCCS designs utilize a tall chimney to enhance the driving head needed for natural circulation. However, the reliance on a tall chimney also contributes to a higher likelihood of flow instabilities [3]. One of the most widely studied flow instabilities is the flashing-induced instability [4]. It typically happens when flashing occurs at the top of an unheated chimney, causing a reduction in the hydrostatic pressure and an increase in thermal driving head, which then leads to an increase of natural circulation flow rate. As the flow rate increases, the residence time of the fluid in the heated riser decreases and the fluid enters the chimney in a subcooled state. The subcooled fluid suppresses the flashing in the chimney, causing the thermal driving head to reduce and the natural circulation flow rate to decrease, leading to an increase of residence time of the fluid in the riser, and eventually the repeat of the process [5].

Other types on instabilities typical in a low-pressure natural circulation boiling system include natural circulation oscillations, density wave oscillations (DWOs), and geysering [6]. Using the SIRIUS-N facility, Furuya et al. [6] found that DWOs were the cause of the induced flow instabilities by studying the flow oscillation period and the fluid transit time through the chimney. With a scaled test facility that consisted of a two parallel boiling channels, Chiang et al. [7] performed fundamental study on the thermal-hydraulic instabilities during start-up in natural circulation boiling water reactors (BWRs). Three types of instabilities were reported from their study, namely geysering induced by condensation, natural circulation instability induced by hydrostatic head fluctuation, and DWO. Using the CIRCUS facility in both single-chimney and two-parallel chimney configurations, flashing induced-instability was investigated by Marcel et al. [8,9]. It was reported that the only type of instability observed in the single-chimney configuration was DWOs while geysering and DWOs were both observed in the two-parallel chimney configuration. In addition the studies mentioned here, experimental investigation of two-phase instabilities in natural circulation have been widely conducted using different facilities under various conditions. A comprehensive summary of these studies can be found in the work by Zhao et al. [5], Zhang and Brooks [10], and Ruspini et al. [11]

Given the advancement of computational capabilities in recent years, computational models have been increasingly utilized by researchers to study various designs of RCCS. Due to their fast running speed and low requirement of computational resources, system-level codes are the tool of choice for many previous studies. Among them, RELAP5 is one of the most widely used computational codes. As highlighted by Shi et al. [12], RELAP5 is recognized as one of the top estimate system analysis codes and has been selected for the simulation of the natural circulation flow driven systems by many researchers. Furthermore, according to Bertodano et al. [13], RELAP5 is capable of modeling global instabilities particularly DWOs. Some recent studies that used RELAP5 to investigate instabilities in natural circulation include the works by Zhao et al. [5] who observed different oscillation patterns in flashing-induced instabilities in natural circulation system. The authors also studied the effects of parameters such as inlet subcooling, system pressure, inlet resistance, and chimney height on the instabilities. Shi et al. [12] used experimental data to assess the capability of RELAP5 in predicting the startup transients in a natural circulation test facility simulating a BWR-type Small Modular Reactor (SMR). The study found that despite some discrepancies in

the timing of the system pressure, the code can predict the natural circulation flow velocity relatively well. Shi et al. [12] also mentioned that the simplification of the RELAP5 nodalization and the neglect of heat loss and other local three-dimensional effects could lead to uncertainties in the predictions. Wang et al. [14] conducted natural circulation flow instability experiments and used RELAP5 to analyze the four oscillations observed in the experiments, namely intermittent and periodical oscillation, double-peak oscillation, periodical sinusoidal oscillation, and staged irregular oscillation. An excellent agreement was obtained between the simulation and the experimental data for intermittent oscillation and sinusoidal oscillation. The authors suggested that the deviation between the simulation and the experimental result was likely due to the non-linear relationship between the natural circulation driving force and kinetic energy. Teng et al. [15] evaluated the applicability of RELAP5 to simulate flow instability in a natural circulation system using the experimental data from the NHR-200 test facility. The authors reported that RELAP5 was able to simulate DWOs in the test facility where the interphase friction correlation and the resistance models played a major role in the accuracy of the prediction.

In addition to investigating general flow instabilities, RELAP5 has also been adopted by researchers in studying the behavior of various designs of RCCS. These studies include Lomperski et al. [16] who used the code to model the air-cooled RCCS of the GA-MHTGR design to confirm the scaling laws used for designing the NSTF, Corradini et al. [17] who performed single and two-phase simulations on a scaled facility with three riser channels to investigate the behavior of the system as it transitioned to two-phase flow in a natural circulation mode, and Vaghetto and Hassan [18] who used the code to study the behavior of a small scale experimental RCCS facility during steady-state and ramp-up phase.

Within the NSTF program, computational and simulation efforts have also been established with the objectives to develop mature and well-tested computational models to simulate the NSTF, to validate and verify computer codes and simulation tools with the experimental data, and to assist the experimental team by providing insights from the simulations. Under this campaign, system-level analyses are performed first with RELAP5-MOD3.3 and later with RELAP5-3D to investigate loop-wide behaviors during long transients while CFD simulations are conducted to study local flow behaviors in high details [19]. As discussed above, many past system-level simulations of RCCS focused on single-phase flows, steady-state cases, or simplified transient cases. In attempting to expand the availability of RCCS-related computational works in the literature, this paper presents some of the simulations performed under the NSTF campaign using RELAP5-3D, emphasizing on the simulations of a fault condition where the natural circulation in the RCCS is disrupted. A detailed analysis of the simulation results is provided where they are compared with the experimental data acquired by the NSTF experimental team. In the coming sections, the NSTF facility is briefly discussed, followed by a description of the RELAP5-3D model. For the simulation results, a short discussion on the two-phase baseline simulation is provided with the remainder of the discussion focused on the simulations of a fault condition where the riser header inlet flow area is gradually reduced.

2. Methodology

2.1. Experimental facility

The NSTF reflects a 1/2 axial scale and 12.5° sector slice of the primary design features of a full scale RCCS concept for the Framatome 625 MW_t SC-HTGR, with a total height of 18.1 m in its current configuration. The main components of the facility include a closed cavity heated by electric heaters, an eight-riser cooling panel test section, and a water tank that are connected with a series of piping to form a closed loop. The schematic of the NSTF is shown in Fig. 1. The flow direction is represented by the blue arrows where water is heated along the heated

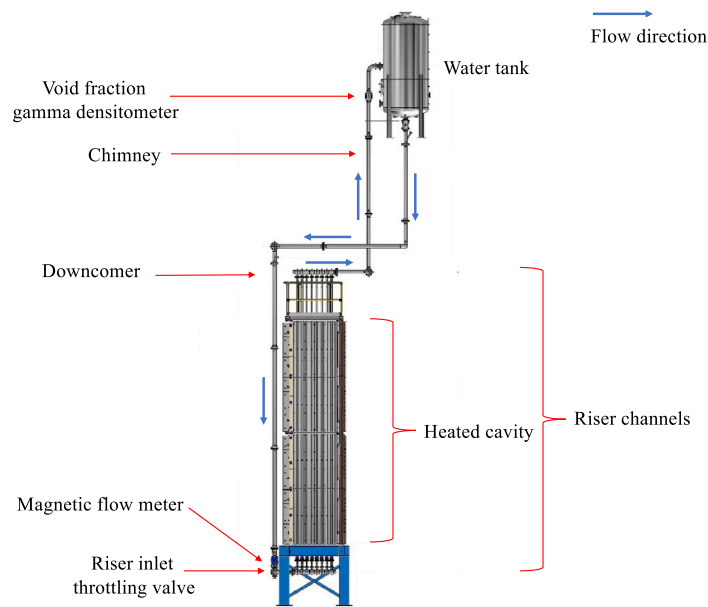


Fig. 1. Side view of the schematics of the water-based NSTF.

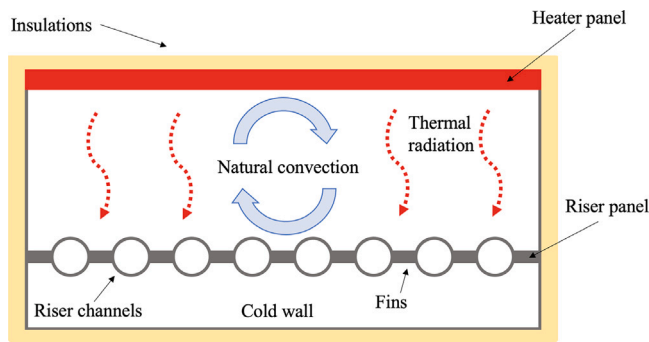


Fig. 2. Top views of the NSTF cavity.

section of the test section, rises through the chimney, enters the tank from the side wall, and flows back down through the downcomers and back at the riser inlet. On the other hand, the schematics of the riser channels with the fins and the cavity are shown in Fig. 2. The cavity consists of a heater panel, two side walls, a top wall, a bottom wall, and a back wall. It is divided into a hot side and a cold side by the riser panel which is located 0.865 m from the heater panel. Thermal radiation and natural convection are the two primary heat transfer mechanisms between the heater panel and the riser panel as well as the other walls. Further information on the design and instrumentation used in the test facility can be found in a series of reports published by the NSTF team [20–23].

2.2. RELAP5-3D model description

The system-level modeling of the NSTF is performed with RELAP5-3D version 4.3.4 [24]. In this work, the model of the NSTF can be broken down into the primary loop and the cavity. The primary loop consists of the riser channels, water tank, and the piping network while the cavity is defined as the enclosure surrounded by the heater panel, the riser panel, and the unheated panels. A reference RELAP5 model for the primary loop NSTF has previously been developed by Lv et al. [25]. The nodalization diagram of the model for the primary loop of the facility is shown in Fig. 3. The inlet and outlet headers of the riser tube assembly in the water-based NSTF are fabricated from a set of

tees, which are modeled as branches in the present model, namely, B790–B720 and B590–B520. A total of eight risers are modeled, each consisting of an upstream non-heated region (P691–P698), a heated region (P671–P678), and a downstream non-heated region (P651–P658). The riser tube assembly is connected back to the water tank through pipes of P450–P490 while the outlet of the tank is connected to the inlet of the riser assembly via the downcomer modeled as P840–P890. All the piping is made of 4.0" Schedule 40 pipes, with an ID of 0.1033 m.

The water tank is modeled as three different volumes, namely a branch (B969) and two pipes (P950, P980). The branch-component represents the thermal-mixing water region, while the pipes represent the bottom half of the tank, and the air/stream region, respectively. All the piping/tank walls are modeled as heat structures, with convective boundary condition for the inner surface. To model the heat loss, 2-inch-thick K-FLEX thermal insulation is modeled as part of the heat structures, and a natural convective heat loss boundary condition is applied to the outer surface. In two-phase analysis of this work, the active-cooling component is removed so water is allowed to boil off and steam is discharged from the system to the environment.

The cavity of the NSTF, shown in Fig. 2, consists of the eight riser tubes with the fins, the two side walls, the heated plate, and the top and bottom walls. The model of the cavity has previously been developed in the work by Lv et al. [19] and is adopted in this work. The schematic of the cavity model is shown in Fig. 4. The two main heat transfer mechanisms in the cavity are natural convection and radiative heat transfer. For radiative heat transfer, the riser assembly, heated plate, and the side walls are each axially divided into eight vertical layers, resulting in a total of 98 surfaces that are modeled within one radiation enclosure. The required inputs of view factors are calculated from CFD simulations [19]. On the other hand, for the internal natural convection, results from CFD analysis show that the flow is predominantly confined to regions next to the panels [25]. Hence, the flow of natural convection in the cavity is modeled with flow channels with the flow area determined by the CFD analysis. Note that in Fig. 4, the flow path of natural convection in the cavity is modeled with components 100 to 105. Components 103 and 104 represent the flows at the top and bottom panels of the cavity, components 101 and 102 represent the flows at the side panels, component 100 represents the flow at the heated panel, and component 105 represents the flow at the riser panels.

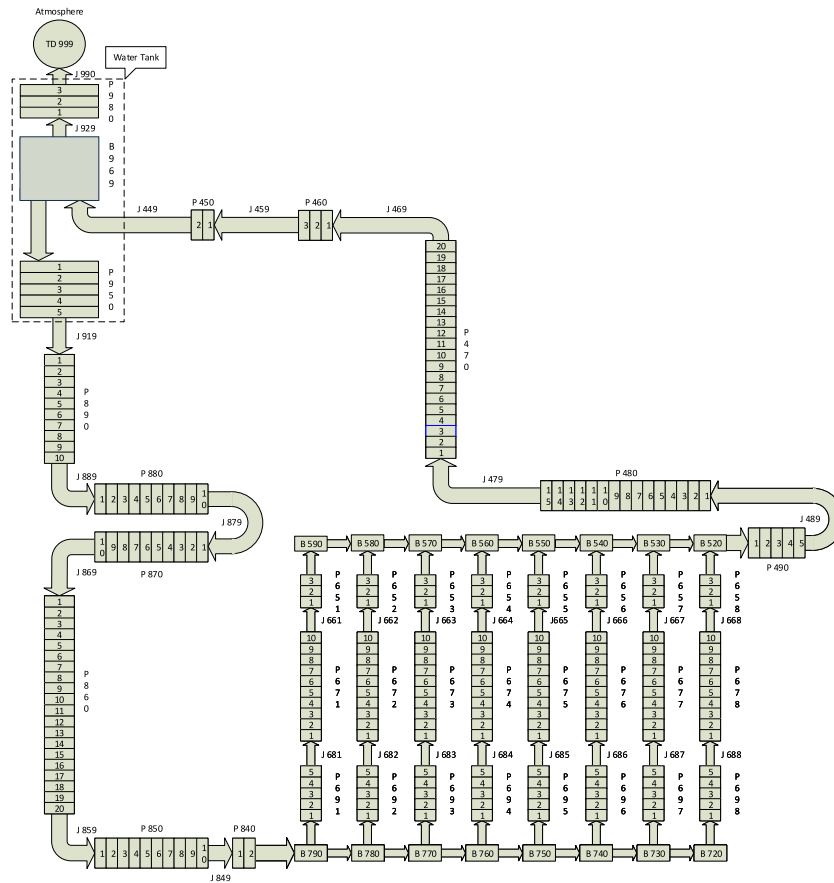


Fig. 3. The nodalization diagram of the RELAP5-3D model for the primary loop.

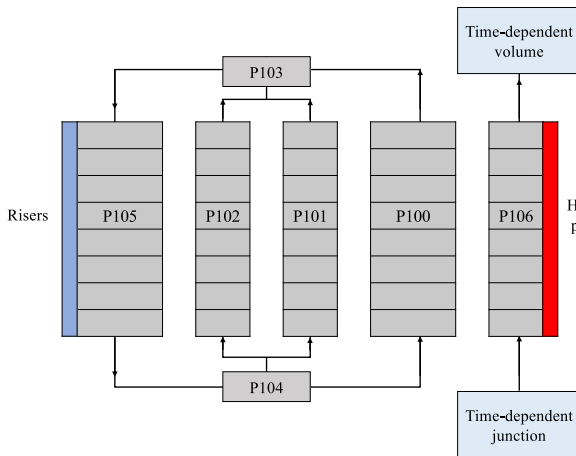


Fig. 4. The nodalization diagram of the RELAP5-3D model for the cavity.

In the NSTF, adjacent risers are connected by fins to form a panel. Heat transferred to the fins is transferred to the riser walls via conduction and eventually to the water flowing in the risers via convection. In RELAP5-3D, conductive and radiative heat transfers are modeled using the enclosure system. However, each heat structure surface cannot be specified in more than one enclosure, thus some assumptions are necessary to overcome this limitation while keeping the model as accurate as possible. In this work, the fin and the riser are modeled as one heat structure where the heat conduction from the fins to the riser walls are neglected. This assumption is justifiable because the conduction

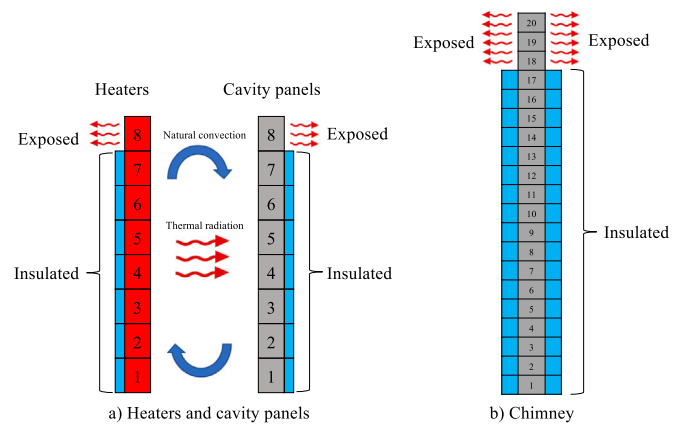


Fig. 5. The ad-hoc approach to improve the prediction of heat loss experienced by the (a) heaters and cavity panels and (b) the chimney.

resistance is much smaller than that of the radiation. Similar approach was adopted by Vaghetto and Hassan [18] in their work modeling a similar facility with RELAP5-3D. The specific heat capacity of the riser walls is also adjusted to account for the missing heat capacitance of the fins. Note that the cold side of the cavity is not included in the model as CFD analysis shows that the temperature on the cold side is significantly lower by more than 150 °C and is considered to have little effects on the heat transfer on the hot side [25]. Given the low significance of the cold side, including it to the model will increase the complexity of the model and create further uncertainties. The same simplification was also applied by Vaghetto and Hassan [18] using the same justification.

The heater panel consists of a stainless-steel plate, ceramic heaters, multiple layers of insulation, and an air gap between the heated plate and the heaters. Heat losses due to air flow in the gap between the heated plate and the ceramic heaters as well as the radiative heat transfer between these two surfaces are modeled, represented by component 106 in Fig. 4. Heat loss due to natural convection on the outer surface of the cavity walls is also considered in the model by specifying the heat sink temperature and temperature-dependent heat transfer coefficients.

Based on previous study [26], it was discovered that heat loss is underestimated by the RELAP5 model and resulted in inaccurate prediction in the two-phase region. Although the NSTF is insulated, it is deduced that heat can still escape to the environment through the support structures or instrumentation mounts, which are not included in the RELAP5 model to keep the model reasonably simple. Furthermore, it is challenging to quantify the amount of heat loss experienced by the entire facility, given the size and the complexity of the NSTF. As a result, in order to improve the prediction of heat loss experienced by the facility while maintaining the simplicity of the model, an ad-hoc approach is adopted where the insulation at the top-most nodes of the heaters and the cavity panels are removed. This approach provides a direct path for heat to escape from the heater and the cavity to the environment. Using the difference between the heat produced by the heater and the heat entering the water flow in the primary loop through the risers, the heat loss experienced by the cavity can be approximated. The heat transfer coefficients of the exposed surfaces are then tuned until the calculated heat loss of the model matches the experimental value. Similar approach is also applied to the upper section of the chimney in the model as it was learned from previous work that the heat loss experienced by the chimney could have a significant impact on the two-phase prediction [27]. Details on this approach and its improvement to the RELAP5 predictions are available in the report by Ooi et al. [27]. An illustration of the ad-hoc approach is shown in Fig. 5. It must be stressed that such an ad-hoc approach is necessary because one of the primary objectives of this work is to assess RELAP5-3D's ability to predict two-phase flows and instabilities. By minimizing the uncertainties due to inaccurate modeling of heat loss, the analysis can be focused on understanding the two-phase predictions by the code. Nevertheless, it should be mentioned that the ad-hoc approach invariably introduces some uncertainties to the simulation results. However, the uncertainties cannot be quantified due to the lack of heat loss experimental data from the test facility. Should heat loss data be available in the future, the ad-hoc approach will be revisited to better investigate its uncertainties. Lastly, given that two-phase instability is a relatively fast transient, the time steps of the simulation are limited to a maximum size of 0.1 s.

Given that this work focuses on flashing induced instability, the models used for calculating the vapor generation rate under flashing flows are briefly mentioned here. In general, the vapor generation rate in RELAP5-3D is dictated by the volumetric interfacial heat transfer coefficient which is calculated with flow regime-based correlations. This work uses the default models in RELAP5-3D for calculating the volumetric interfacial heat transfer coefficient. According to the RELAP5-3D theory manual [24], in bubbly flow, the volumetric interfacial heat transfer coefficient is calculated as the maximum between the Plesset-Zwicky correlation [28] and the modified Lee-Ryley correlation [29] with an additional term to represent enhanced nucleation effects at a low void fraction condition following a pressure undershoot. For slug flow, the volumetric interfacial heat transfer coefficient is the sum of (1) the heat transfer between the large Taylor bubbles and the surrounding liquid and (2) the heat transfer between the small bubbles at the surrounding liquid [24]. For the Taylor bubble, the volumetric interfacial heat transfer coefficient is calculated with an ad-hoc correlation that is a product of a large coefficient, void fraction, and volumetric interfacial area [24]. The large coefficient is added to promote a rapid return of liquid temperature towards the saturation temperature. Meanwhile, the vapor generation rate due to heat transfer

between the small bubbles and the surrounding liquid is calculated with the same correlations as that in the bubbly flow.

For annular mist flow, interfacial heat transfer results from (1) the heat transfer between the annular liquid film and the vapor core and (2) the heat transfer between the entrained liquid droplets at the vapor core. The volumetric interfacial heat transfer coefficient for the former is also calculated with an ad-hoc correlation with of a similar form as that of the Taylor bubble. The ad-hoc correlation also has a large numerical coefficient to artificially push the fluid temperature toward the saturation temperature. Similarly, the volumetric interfacial heat transfer coefficient of the entrained liquid droplets also has a function designed to grow quadratically with superheat for the same purpose. For horizontally stratified flow which exists in the horizontal pipe between the chimney outlet and the tank inlet, the volumetric interfacial heat transfer coefficient is calculated with an ad-hoc correlation that accounts for the heat transfer between the flat liquid interface and the vapor as well as that between the entrained droplet interface and the vapor. The correlation also artificially enhances the value of the volumetric interfacial heat transfer coefficient to promote the return of the liquid temperature to the saturation temperature. Readers are directed to the RELAP-3D theory manual [24] for detailed derivations and discussions on the correlations.

3. Results and discussions

3.1. Two-phase baseline case

In this section, the results from the RELAP5-3D simulations are analyzed and discussed. The results are compared to the experimental data by Lisowski et al. [22]. Run057, a two-phase transient case, is selected as the baseline case with which the RELAP5 model is benchmarked. The baseline case is only briefly discussed here for completion as a detailed discussion has already been provided by Ooi et al. [27]. In Run 057, the water in the system is heated with a thermal load of 51.6 kW_t, equivalent to 2.1 MW_t in the full-scale RCCS by Framatome. The initial tank inventory is set to 80%. The heater power is applied across a 90-minute linear power ramp and then is maintained constant to allow the heating up of the NSTF facility and water inventory. Upon reaching saturation, boiling/flashing of water is first observed in the upper chimney region, and sustained for over 4 hours, followed by power ramp down. Note that the power ramp down is not included in the RELAP5 model for simplicity. The secondary cooling system is excluded from the RELAP5 model and vapor is discharged directly to the environment. For more details on Run057 such as the experiment procedures and measurement uncertainties, readers are directed to the report by Lisowski et al. [22].

Fig. 6(a) shows the comparison between the experimental and predicted system mass flow rates for Run057. The mass flow rate in Fig. 6 can be divided into a single-phase region that happens between the start of the experiment to approximately hour-13 and a two-phase region that happens from hour-13 onward. As the heater power is ramped up, water in the riser channels are heated which provides the thermal driving head to drive the natural circulation in the main loop of the NSTF. As water is continuously heated in the riser channels, its temperature eventually rises above the local saturation temperature at the top of the chimney and the tank. At this point, boiling/flashing occurs where a significant amount of void (vapor) is generated near the chimney exit. Flashing-induced natural circulation instability ensues where large flow oscillations are observed. The generation of void near the chimney exit causes a larger thermal driving head from density difference between the riser and downcomer, which leads to an increase of flow rate. The higher flow rate reduces the residence time of water in the riser channels thus lowering the temperature of water entering the chimney. As the colder water remains subcooled near the chimney exit, flashing ceases, the thermal driving head reduces, and the flow rate decreases. The slowing of flow increases the residence time of

water in the risers and allows it to be heated to a higher temperature as it enters the chimney. This once again leads to flashing at the top of the chimney as the water temperature is now higher than the local saturation temperature. The entire process is repeated, resulting in the flow oscillations observed in both the experiment and the simulation.

Good agreement is observed between the experimental and predicted mass flow rates in the single-phase region. Additionally, the overall trend of the two-phase region predicted by the RELAP5 model matches that of the experiment where the oscillations start at approximately hour-13. The model predicts larger oscillation amplitudes that range from more than ± 2.5 kg/s at the beginning to less than ± 0.3 kg/s near the end of the instability. On the other hand, despite the large initial spike, the oscillations in the experiment have smaller amplitudes that range from roughly ± 1.5 kg/s to ± 0.2 kg/s. In both cases, the amplitudes of oscillations are observed to decrease as the oscillations progress. At approximately hour-17, the flow transitions to a quasi-steady two-phase region where the flow oscillates at a relatively uniform amplitude for an extended period. However, the RELAP5 model predicts a complete stabilization of flow at roughly hour-18.5, which is not observed in the experiment.

Fig. 6(b) compares the chimney exit void fraction from the experiment and the RELAP5 model. In the single-phase region, the experimental and predicted void fractions are zero, with the former showing occasional small spikes that are likely due to noise in the gamma densitometer measurement. In the two-phase region, the amplitudes of oscillations from both sets of results are similar till roughly hour-14.5. Beyond that, the trends begin to diverge where the predicted void fraction appears to converge to roughly 0.4 in the quasi-steady two-phase region. Conversely, the experimental void fraction converges to a smaller value of only 0.1. This difference could be due to the overprediction of vapor generation rate by the RELAP5 model, which has been reported by other researchers [30–32]. As described in the RELAP5-3D theory manual [24], the flashing vapor generation rate is computed as a function of the volumetric heat transfer coefficient, H_{if} . For slug flow, the volumetric heat transfer coefficient is calculated as the sum from the interfacial heat transfer between the Taylor bubbles and the surrounding liquid as well as that between the spherical bubbles and the surrounding liquid. For the Taylor bubble, the volumetric heat transfer coefficient is determined from an ad-hoc correlation defined as $H_{if} = 3.0 \times 10^6 a_i \alpha_g$, where a_i and α_g are the volumetric interfacial area and void fraction of Taylor bubble, respectively. The ad-hoc correlation has a large coefficient to artificially enhance the interfacial heat transfer in order to promote the rapid return of liquid temperature to the saturation temperature. It is likely that this artificial enhancement of the volumetric heat transfer coefficient is the cause of the overprediction of void fraction at the chimney exit. As stated by Mangal et al. [33] who performed RELAP5 simulations to study natural circulation in a high pressure natural circulation loop and a parallel channel loop, the questionable applicability of these semi-empirical constitutive relations in different flow conditions could be one of the causes of the inaccuracy of the code. Furthermore, the higher predicted void fraction in the quasi-steady two-phase region likely leads to a higher predicted mass flow rate due to larger thermal driving head caused by density difference between the riser and downcomer.

Fig. 7(a) compares the tank gas space pressures from the experiment and the RELAP5 model. Overall, the trends from both sets of results are similar where the pressure remains constant at atmospheric pressure in the single-phase stage. As the flow transitions into two-phase due to flashing in the tank and upper chimney, the accumulation of vapor in the tank gas space causes the pressure to increase. At roughly hour-17, the pressures reach the maximum value and start to stabilize. The predicted pressure appears to be consistently lower than the experimental value by approximately 2 kPa. Fig. 7(b) compares the chimney outlet pressures from the experiment and the model. The chimney outlet pressure is roughly 10 kPa higher than the tank gas space pressure due to additional hydrostatic head. The overall trends of the experimental

and predicted chimney outlet pressures also match those of the tank gas space pressure. Similarly, the predicted pressure at the quasi-steady two-phase region is lower than the experimental value by less than 5 kPa.

Table 1 summarizes the comparison between the experimental data and the RELAP5-3D predictions for Run057. Note that average values are used in the two-phase region due to the oscillations. The overall comparison between the two sets of data are relatively good especially during single-phase where the mass flow rate and pressures are almost identical. Similarly, the agreement of the mass flow rate and pressures in the quasi-steady two-phase region, roughly between hour-17 to hour-19, between the two sets of results is generally good. The only exception is the chimney outlet void fraction where RELAP5-3D predicts a value of 0.4 while the experimental data shows a value of only 0.075. Additionally, the average oscillation periods are tabulated where the oscillations are divided into an unsteady stage and a quasi-steady stage. In both stages, the experimental periods are observed to be greater at 187.2 s and 152.2 s, respectively, compared to the predicted values of 141.7 s and 113.8 s, respectively.

Fig. 8 compares the mass flow rate predicted by the RELAP5-3D model with 20, 40, and 60 nodes for the chimney. It is observed that the predicted mass flow rates in the single-phase stage are almost identical for the different numbers of nodes. On the other hand, some differences are observed in the two-phase stage. At higher number of nodes, the two-phase oscillatory region appears to have a cone-line shape followed by a long and thin quasi-steady region. Conversely, at 20 nodes, the two-phase oscillatory region exhibits a more gradual reduction of oscillation amplitude, which is closer to the observation from the experiment. Given the similarity between the experiment and the simulation in terms of the overall shape of the two-phase oscillatory and quasi-steady regions, the number of nodes in the chimney is set to 20.

3.2. Fault condition - Reduction of riser header inlet flow area

Based on the discussions in Section 3.1, it is seen that the RELAP5-3D model is able to predict the experimental two-phase baseline case relatively accurately. Provided that heat loss is accounted for correctly, the predicted onset, amplitude, and length of flow oscillations show good agreement with the observations from the experiment. In this section, the validation of the model is extended to a fault condition where the flow area of the riser header inlet is gradually reduced. The fault condition represents one possible scenario in the RCCS where debris accumulation occurs at the inlet of the risers.

To study the effects of the reduction of riser header inlet flow area, a pneumatically controlled 4.0 " nominal sized full-bore ball valve is installed at the upstream of the riser header. The flow area of the valve is 8.213×10^{-3} m² when fully open. The valve can be controlled across the entire range of positions, from fully open to fully closed. The prediction by the RELAP5-3D model is compared with the experimental data from Run071 by Lv et al. [23].

This test utilized a continuous refill of boil-off condensate back into the loop to ensure that the loop operates at a true thermal and hydraulic steady-state mode of operation. The condensate refill system maintains a constant inventory level inside the water tank by manually adjusting the refill rate to match the steam/condensate generation rate. For the RELAP5-3D model, the heat removal system on the secondary side is not modeled. Instead, a simple time-dependent junction is added to the tank to supply water at the measured condensate temperature from the test back to the tank where the mass flow rate of the feed water is equal to the vapor discharge rate from the tank.

Once the facility reached a two-phase thermal and hydraulic steady-state condition ten stages of inlet restriction were imposed on the operating test loop, beginning with fully open to severely restricted. The summary of the stages is included in Table 2 along with the

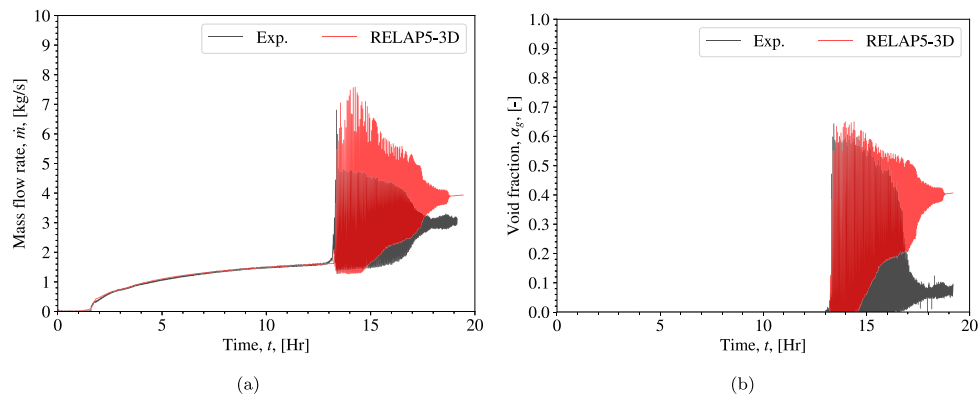


Fig. 6. Comparison of the experimental and predicted (a) system mass flow rate and (b) chimney outlet void fraction for Run057.

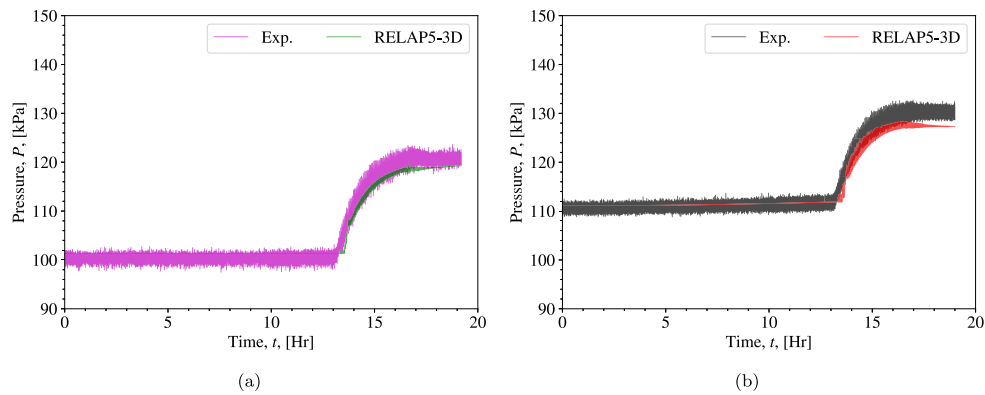


Fig. 7. Comparison of the experimental and predicted (a) tank gas space pressure and (b) chimney outlet pressure for Run057.

Table 1

Summary of the comparison between the experimental data and RELAP5-3D predictions for Run057.

	Units	Experiment	RELAP5-3D
Single-phase mass flow rate (before boiling inception)	kg/s	1.6	1.6
Single-phase chimney outlet pressure	kPa	111.0	111.0
Single-phase tank gas space pressure	kPa	100.0	101.8
Quasi-steady two-phase mass flow rate	kg/s	3.0	4.0
Quasi-steady two-phase tank gas space pressure	kPa	121.0	119.0
Quasi-steady two-phase chimney outlet pressure	kPa	130.0	126.5
Quasi-steady two-phase chimney outlet void fraction	–	0.075	0.4
Unsteady oscillation period	s	187.2	141.7
Quasi-steady two-phase oscillation period	s	152.2	113.8

loss coefficients, K . Note that the flow areas of the valve at different valve positions are estimated based on the valve geometry and design information from the manufacturer. The loss coefficients are obtained through the pressure drop measurements across the valve and defined based on the velocity at full valve flow area. More information regarding this process can be found in the report by Lv et al. [34].

Fig. 9 compares the experimental and predicted system mass flow rate for the inlet throttling case. The experimental and predicted results are represented by the black and red solid lines, respectively. Furthermore, a dashed green line representing the opening of the valve, with one being fully open and zero being fully closed, is added to show the stages of the experiment.

The experiment shows that as the valve is closed from stage-1 to stage-3, the oscillations start to diminish until they are completely dampened from stage-4 to stage-6 and the flow transitions into a stable two-phase flow. The dampening of flow oscillations by increasing the inlet loss coefficients is well known and has been reported by many previous studies such as the work by Furuya et al. [35]. At the same time, the overall flow rate also decreases as the valve is closed. Lv et al. [23] stated that the oscillations experienced by the facility thus

Table 2

Loss coefficients of the throttling valve at the riser header inlet.

Stages	Averaging window (Hr)	Flow area (%)	Flow area ($\times 10^{-3} \text{ m}^2$)	K
1	15.83 – 16.13	100.0	8.213	0.05
2	16.13 – 16.50	75.0	6.160	1.78
3	16.50 – 16.85	60.0	4.928	8.02
4	16.85 – 17.17	50.0	4.107	23.04
5	17.26 – 17.53	40.0	3.285	69.85
6	17.60 – 17.88	36.7	3.014	105.19
7	17.88 – 18.23	33.4	2.743	159.54
8	18.31 – 18.57	30.0	2.464	262.92
9	18.62 – 18.92	27.5	2.259	379.13
10	19.02 – 19.26	25.0	2.053	653.36

far are due to flashing in the upper section of the chimney. The increase of driving force from flashing in the chimney causes a rise in the flow rate which in turn reduces the residence time of liquid in the heated section of the risers. This decreases the liquid temperature entering the chimney and suppresses the flashing occurring near the top of the chimney. As a result, the driving force is reduced and the liquid

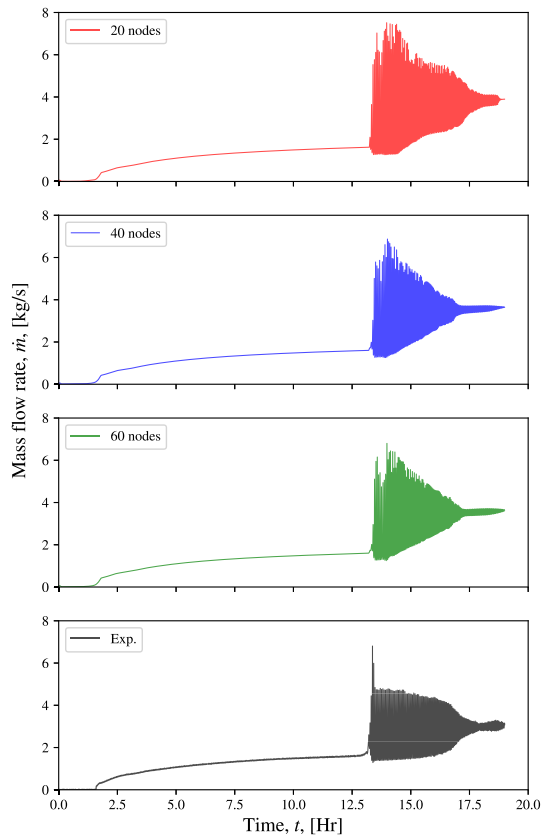


Fig. 8. Comparison of the predicted mass flow rate for Run 057 with different numbers of nodes in the chimney.

temperature entering the chimney once again increases, leading to the repetition of the process.

At stage-7 with the flow area at 33.4%, oscillations are reintroduced. According to Lv et al. [23], the oscillations at this stage are of a different type compared to the oscillations in previous stages. The oscillations observed in stage-7 appear to be irregular and have jagged curves compared to the smooth sinusoidal shaped flashing induced oscillations seen in the previous stages. Lv et al. [23] suggested that these could be Type-II density wave oscillations (DWO) due to multiple regenerative feedbacks between the flow rate, vapor generation rate and pressure drop. As the valve is further closed from stage-8 and stage-9, the DWOs are dampened and the flow is once again stabilized.

Finally, at stage-10 with the valve area at only 25%, oscillations once again reappear. The oscillation pattern appears to be different from the flashing and DWO instabilities observed in previous stages. The oscillations at stage-10 are more chaotic and the flow rate is observed to drop below zero, indicating the occurrence of flow reversal. According to Lv et al. [23], the flow restriction imposed by the valve at this stage increases the residence time of the fluid in the heated section and leads to boiling in the risers. At the same time, the high fluid temperature allows the fluid to reach saturation temperature before rising through the chimney. The combination of events leads to the onset of the parallel channel instability (PCI) that causes independent voiding and flow excursions across the parallel riser channels. PCI results from the influences of flashing, boiling, and geysering, and is chaotic in nature with random flow reversals in individual channels.

The RELAP5-3D prediction is somewhat different from the experimental observation. With the closing of the valve at stage-2 and stage-3, the oscillations are significantly dampened and the flow rate is reduced. At stage-3, minor oscillations are observed initially but they are dampened out quickly as the condition stabilizes. At stage-4, the closing

of the valve leads to the reintroduction of oscillations with further reduction of flow rate. The initial oscillations appear more irregular and jagged but the oscillations transition into a more regular and sinusoidal pattern once the system stabilizes. The sinusoidal pattern is similar to that observed in stage-1, albeit with a larger amplitude, suggesting that these are likely flashing driven oscillations. The reduction of natural circulation flow rate from the closing of the valve leads to a greater residence time of fluid in the heated riser and causes the fluid to be heated up more, which in turn causes flashing to occur earlier in the chimney. With more intense flashing, the flashing induced oscillations are reintroduced to the system.

As the valve is closed further at stage-5 and stage-6, the flow rate decreases and the oscillations grow. From stage-7 to stage-10, the amplitude of the oscillations decreases as the valve is closed. At the same time, the minima of the oscillations drop below zero, indicating occurrence of flow reversal. Furthermore, the oscillation patterns at these stages appear to be somewhat different from the oscillation patterns at the earlier stages. From stage-7 to stage-10, the rising edges of almost all of the peaks have a minor dip. Similar observations were made by Wang et al. [14] who studied flashing induced natural circulation instabilities with RELAP5. Wang et al. [14] described these as irregular but periodical oscillation. Wang et al. [14] reported this type of oscillations happened during intense boiling in the riser. In the RELAP5-3D model, with further closing of the valve, the natural circulation flow rate decreases and the residence time of fluid in the heated riser increases sufficiently for boiling to occur. Wang et al. [14] suggested that the irregular oscillation pattern is due to the compounding effects from boiling in the riser and flashing in the chimney. The initial increase of flow rate is caused by boiling in the riser, followed by another increase in flow rate due to flashing. The second stage is dominated by flashing, culminating to the flow rate reaching the local peak. The increased flow rate then drives subcooled fluid into the riser which causes the bubbles in the riser to condense and the flow to reverse.

There are some similarities between the oscillations predicted by the RELAP5-3D model and the observations from the experiment. In both cases, the oscillations at stage-1 appear to be flashing induced oscillations. Furthermore, they both show that the closing of the valve can lead to the dampening and stabilization of oscillations, albeit at different stages. It is also observed from the experiment and the model that oscillations can be reintroduced to the flow as the valve is closed further due to the enhancement of flashing. However, there are also some significant differences between the experiment and the prediction. For instance, the model predicts a greater reduction in flow rate that leads to the irregular but periodical oscillations. Conversely, similar chaotic oscillations are only observed at stage-10 of the experiment.

To further examine the oscillations predicted by the RELAP5-3D model, the mass flow rate in the individual riser at each stage is shown in Fig. 10. Note that each plot in the figure represents a stage of the closing of the valve and each colored line in the plots represents the mass flow rate in the individual risers. At stage-1, the oscillations have a sinusoidal pattern that indicates flashing induced instability. At stage-2 and stage-3, the oscillation are dampened and the flow almost stabilize entirely. At stage-4, the oscillations are reintroduced due to the enhancement of flashing in the chimney. From stage-1 to stage-4, the flow rates in the risers appear to be identical. From stage-5 to stage-10, the flow rates in individual risers start to differ. The flow rates appear to be out of sync with respect to each other and exhibit a more chaotic behavior due to boiling in the risers. The uneven distribution of flow across the risers at low flow rates causes the fluid in the risers to reach saturation and boil off at different times, which in turn leads to non-uniform behaviors between the risers.

Fig. 11 compares the experimental and predicted void fractions in the chimney. The black and red solid lines represent the predicted void fractions at the chimney inlet and outlet, respectively, while the blue solid line represents the experimental void fraction near the

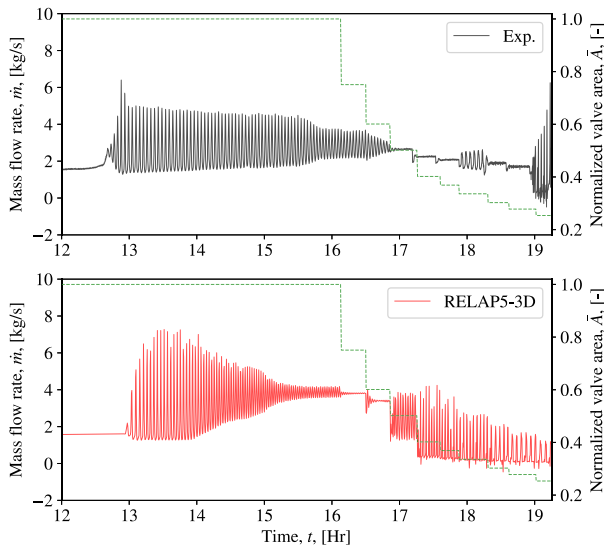


Fig. 9. Comparison of the experimental and predicted system mass flow rate for the inlet throttling case. The green dashed line represents the normalized valve area. (For interpretation of the references to color in this figure legend, the reader is referred to the web version of this article.)

chimney outlet measured by the gamma densitometer. The plots are also partitioned by the green dashed lines into the 10 valve closing stages.

At stage-1, at the outlet of the chimney, the experimental and predicted void fractions show some similarities in terms of the oscillation amplitude where the void fraction oscillates between zero and 0.6. However, the predicted void fraction slowly edges upward to an average value of 0.4 while the experimental value shows a downward trend and oscillates around a value of 0.2. From stage-4 onward, the experimental and predicted void fraction at the chimney outlet are somewhat different. In the experiment, it is observed that the closing of the valve from stage-4 to stage-6 produces a dampening effect on the oscillations and simultaneously causes the overall value of the void fraction to increase. At stage-7 where the system is thought to be undergoing DWO, the oscillations return before stabilizing once again at stage-8 and stage-9. At stage-10, the void fraction shows large oscillations initially before dampening slightly as the system undergoes PCI. On the other hand, for the prediction, as the valve is closed at stage-2 and stage-3, the oscillations in the chimney outlet void fraction start to dampen as seen in the predicted flow rate in Fig. 9. This is similar to the observation in the experiment from stage-4 to stage-6. At stage-4, with the enhancement of flashing and the reintroduction of oscillations, the predicted chimney outlet void fraction is observed to undergo large oscillations spanning from zero to almost one. As the valve is closed further, the oscillations of the chimney outlet void fraction intensifies. The predicted void fraction at the chimney inlet is also shown. Note that there is no comparison with the experimental value because void fraction is not measured at the chimney inlet in the experiment. The predicted void fraction at the chimney inlet is zero from stage-1 to stage-4. However, at stage-5, predicted void fraction starts to become non-zero due to boiling in the risers. This coincides with the flow rate in risers becoming out-of-sync with each other as shown in Fig. 10. Further closing of the valve from stage-6 onward intensifies the boiling in the risers which results in larger amplitudes of oscillations in the chimney inlet void fraction. Similar pattern of oscillations of the chimney inlet and outlet void fraction was reported by Zhao et al. [5] who performed RELAP5 simulation to study flashing-induced instabilities in a natural circulation system.

It should be mentioned that in the current work, the predicted chimney outlet void fraction peaks at 0.9973. This indicates that the

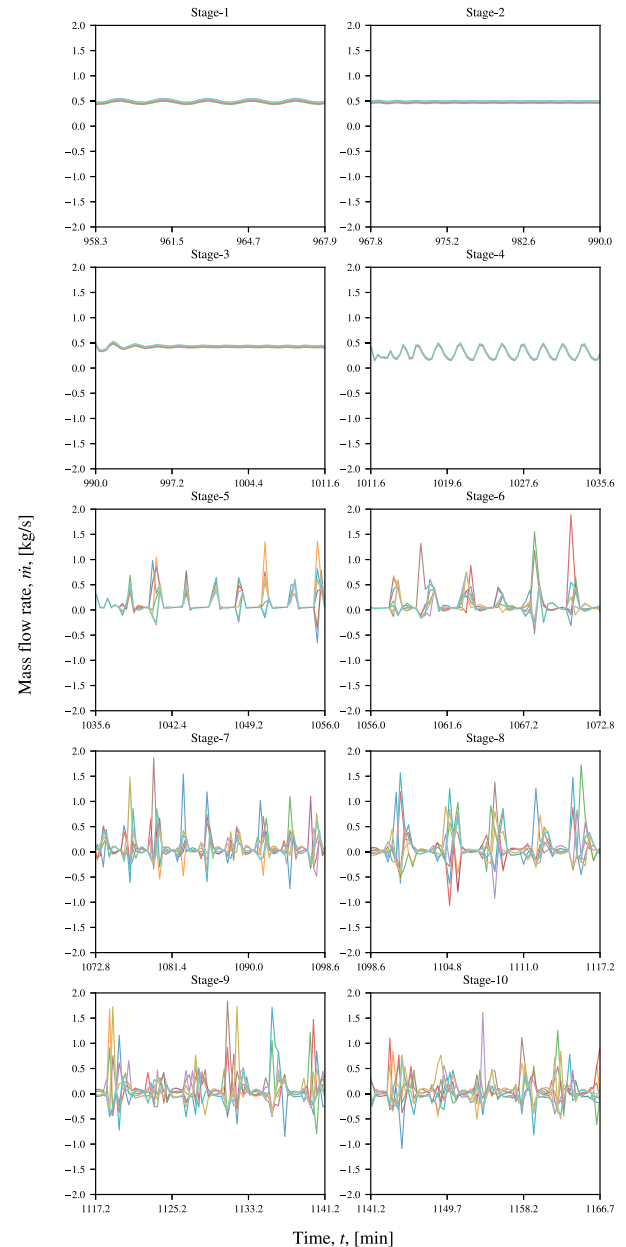


Fig. 10. Comparison of the individual riser mass flow rate predicted by the RELAP5-3D model for the inlet throttling case. Each plot represents a valve stage and each line in the plot represents the mass flow rate in an individual riser.

flow is annular mist at the exit of the chimney because the upper limit of the annular mist regime is set to 0.9999 in RELAP5-3D [24]. Nevertheless, the use of RELAP5-3D to model such high void fraction oscillatory conditions should be proceeded with caution as they could be close to the numerical limit of the code.

The flow regime at various elevations predicted by the RELAP5-3D model is shown in Fig. 12 with Vol-1 being the chimney inlet and Vol-20 the chimney outlet. In the plots, single-phase and bubbly flow are represented as 4, slug flow as 5, annular mist as 6, and pre-CHF mist as 7. The chimney inlet remains at single-phase through the first four stages, in agreement with the predicted void fraction shown in Fig. 11. As the valve is closed from stage-5 to stage-7, the flow transitions into slug flow initially and then to annular mist. Further closing of the valve shows that the flow momentarily transitions into pre-CHF mist. This is likely due to the chaotic and random nature of boiling, flashing, and geysering happening at the risers just upstream of the chimney

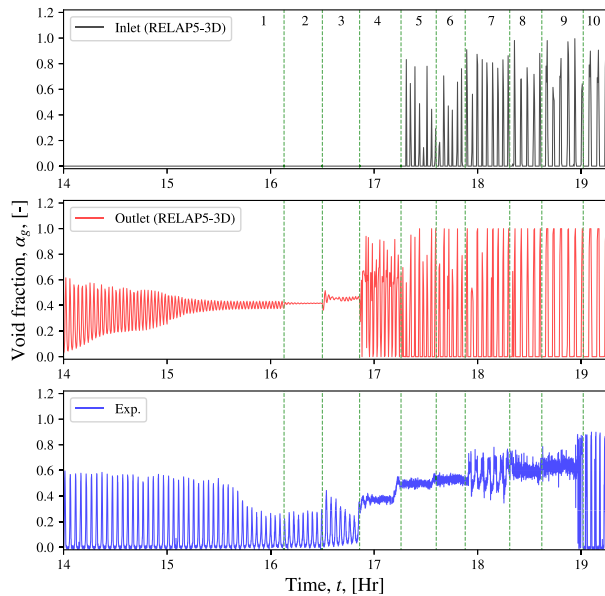


Fig. 11. Comparison of the void fraction in the chimney between the experimental data and the RELAP5-3D predictions. The top figure represents the void fraction at the chimney inlet predicted by the model, the middle figure represents the void fraction at the chimney outlet predicted by the model, and the bottom figure represents the experimental void fraction at the chimney outlet.

inlet. At Vol-10, the flow regime is dominated by annular mist with the occasional transition into slug flow and pre-CHF mist. The closing of the valve appears to somewhat shift the flow regime into pre-CHF mist. The same is true for Vol-15 with the major exception being stage-4 where slug flow is predicted by the model which indicates the occurrence of flashing in Vol-15 at stage-4. Lastly, at Vol-20, the flow is seen to oscillate between single-phase or bubbly flow and slug flow or annular mist. Unlike the lower volumes, pre-CHF mist is not observed in Vol-20. The flow regimes show that the boiling and flashing happening at the risers has a strong influence on the flow regimes near the lower section of the chimney, but not as much at higher elevations. The analysis highlights the complex nature of two-phase flows in an RCCS where the flow could transition between different regimes in a short distance. Any potential effects on heat removal ability due to the transition of flow regimes should be accounted for in the design of an RCCS.

4. Conclusions

This paper presents a system-level RELAP5-3D model of the NSTF, which is a 1/2 axial scale and 12.5° sector slice of the primary design features of a full scale RCCS concept. The objectives of this work are two fold: (a) to extend the system-level modeling of RCCS beyond the steady-state or single-phase domain that are common in the open literature to two-phase and transient domain, (b) to benchmark RELAP5-3D with experimental data generated by the NSTF. A two-phase baseline case is first discussed where the model is able to give good predictions in the single-phase. In the two-phase region, the accuracy of the RELAP5-3D model is mixed. Parameters such as oscillation length, chimney outlet pressure, and tank gas space pressure are predicted well by the model. However, the model overpredicts the void fraction at the chimney outlet, likely due to the overprediction of vapor generation rate by the code. The overprediction of the vapor generation rate is likely caused by the ad-hoc correlation used in RELAP5-3D to compute the volumetric interfacial heat transfer coefficient in Taylor bubbles where a large numerical coefficient is added to artificially drive the fluid temperature back to saturation temperature during flashing. The overprediction of void fraction also leads to the overprediction of mass flow rate in the two-phase region.

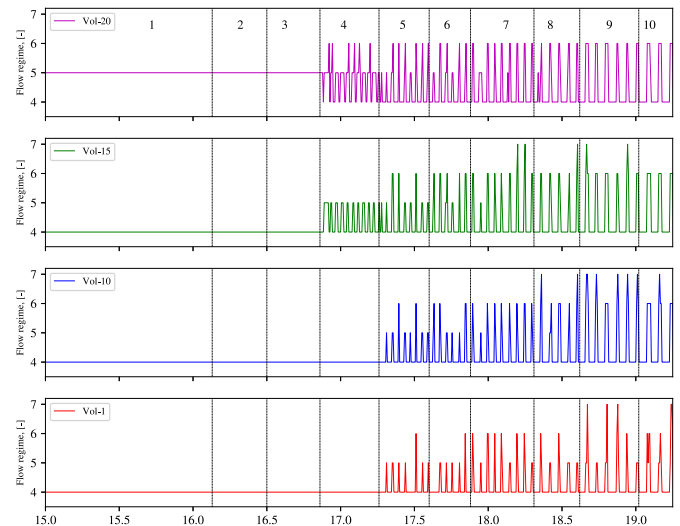


Fig. 12. Flow regimes at various chimney elevations predicted by the RELAP5-3D model. Single-phase and bubbly flow are represented as 4, slug flow as 5, annular mist as 6, and pre-CHF mist as 7.

Majority of the results and discussions presented in this paper are focused on a fault case where the flow area of the riser header is gradually reduced. The fault case is simulated by gradually closing the valve at the riser header inlet where it is observed that the increase of flow resistance at the header inlet has a dampening effect on the flow oscillation in the initial stages. However, further closing of the valve reduces the flow rate and increases the residence time of fluid in the riser, allowing the fluid to be heated up more, which in turn causes an earlier flashing in the chimney. The intensification of flashing in the chimney leads to the reintroduction of oscillations. As the valve is closed further, boiling starts to occur in the riser and the regular and sinusoidal oscillations transition to irregular but periodical oscillations. At the same time, the flow rate appears to fall below zero, suggesting the occurrence of flow reversal. The irregular patterns of the oscillations are due to the compounding effects from boiling in the riser and flashing in the chimney. The predicted oscillations are somewhat different from the experimental observation. The model is able to predict phenomena observed in the experiment such as dampening or stabilization of oscillations, reintroduction of oscillations, geysering and boiling in the risers even though the timeline of these events are not necessarily aligned with that from the experiment. The complex flow regimes in the chimney section is also investigated. Flow regimes such as bubbly flow, slug flow, annular mist, and pre-CHF mist are predicted by the model at various elevation of the chimney. The analysis highlights the complexity of the two-phase flow a water-based RCCS during accident scenarios and the necessity to consider the different flow regimes in the design of an RCCS to ensure that its ability to remove decay heat is remains uncompromised.

The analysis shows that RELAP5-3D is able to predict two-phase oscillatory flows with mixed accuracy. Even though major flow phenomena are predicted by the model, the timelines of these phenomena are not captured well. Furthermore, the overprediction of void fraction in some of the flow conditions can present numerical challenges to the model. As future steps, further examinations on the numerical schemes, closure models, and user options are necessary to improve the overall accuracy of the model. Nevertheless, this work showcases the potential application of RELAP5-3D in the design of an RCCS.

Declaration of competing interest

The authors declare that they have no known competing financial interests or personal relationships that could have appeared to influence the work reported in this paper.

Acknowledgments

This work is supported by the U.S. Department of Energy, Office of Nuclear Energy, Office of Nuclear Reactor Technologies, Advanced Reactor Technologies. The submitted manuscript has been created by UChicago Argonne LLC, Operator of Argonne National Laboratory (“Argonne”). Argonne, a U.S. Department of Energy Office of Science laboratory, is operated under Contract No. DE-AC02-06CH11357.

References

- [1] C. Wang, Y. Liu, X. Sun, P. Sabharwall, A hybrid porous model for full reactor core scale CFD investigation of a prismatic HTGR, *Ann. Nucl. Energy* 151 (2021) 107916.
- [2] D. Lisowski, C. Gerardi, D. Kilsdonk, N. Bremer, S. Lomperski, R. Hu, A.R. Kraus, M. Bucknor, Q. Lv, T. Lee, et al., Final project report on RCCS testing with air-based NSTF, Tech. Rep. ANL-ART-47, Argonne National Laboratory, 2016.
- [3] K. Fukuda, T. Kobori, Classification of two-phase flow instability by density wave oscillation model, *J. Nucl. Sci. Technol.* 16 (2) (1979) 95–108.
- [4] D. Lisowski, O. Omotowa, M. Muci, A. Tokunohiro, M. Anderson, M. Corradini, Influences of boil-off on the behavior of a two-phase natural circulation loop, *Int. J. Multiphase Flow* 60 (2014) 135–148.
- [5] Y. Zhao, M. Peng, Y. Xu, G. Xia, Simulation investigation on flashing-induced instabilities in a natural circulation system, *Ann. Nucl. Energy* 144 (2020) 107561.
- [6] M. Furuya, F. Inada, T. Van der Hagen, Flashing-induced density wave oscillations in a natural circulation BWR—mechanism of instability and stability map, *Nucl. Eng. Des.* 235 (15) (2005) 1557–1569.
- [7] J.H. Chiang, M. Aritomi, M. Mori, M. Higuchi, Fundamental study on thermo-hydraulics during start-up in natural circulation boiling water reactors, (III) effects of system pressure on geysering and natural circulation oscillation, *J. Nucl. Sci. Technol.* 31 (9) (1994) 883–893.
- [8] C.P. Marcel, M. Rohde, T. Van Der Hagen, Experimental and numerical investigations on flashing-induced instabilities in a single channel, *Exp. Therm. Fluid Sci.* 33 (8) (2009) 1197–1208.
- [9] C.P. Marcel, M. Rohde, T.H. Van Der Hagen, Experimental investigations on flashing-induced instabilities in one and two-parallel channels: A comparative study, *Exp. Therm. Fluid Sci.* 34 (7) (2010) 879–892.
- [10] T. Zhang, C.S. Brooks, Linear stability analysis of flashing instability based on the homogeneous equilibrium model, *Nucl. Eng. Des.* 373 (2021) 110994.
- [11] L.C. Ruspini, C.P. Marcel, A. Clause, Two-phase flow instabilities: A review, *Int. J. Heat Mass Transfer* 71 (2014) 521–548.
- [12] S. Shi, Q. Zhu, X. Sun, M. Ishii, Assessment of RELAP5/MOD3. 2 for startup transients in a natural circulation test facility, *Ann. Nucl. Energy* 112 (2018) 257–266.
- [13] M.L. De Bertodano, W. Fullmer, A. Clause, V.H. Ransom, *Two-Fluid Model Stability, Simulation and Chaos*, Springer, 2017.
- [14] Q. Wang, P. Gao, X. Chen, Z. Wang, Y. Huang, An investigation on flashing-induced natural circulation instabilities based on RELAP5 code, *Ann. Nucl. Energy* 121 (2018) 210–222.
- [15] C. Teng, H. Xie, H. Jia, Assessment of RELAP5/MOD3. 2 for simulating density wave oscillation with a two-phase natural circulation test facility, *Nucl. Eng. Des.* 381 (2021) 111358.
- [16] S. Lomperski, W. Pointer, C. Tzanos, T. Wei, A. Kraus, Generation IV nuclear energy system initiative; air-cooled option RCCS studies and NSTF preparation, <http://dx.doi.org/10.2172/1055416>, URL <https://www.osti.gov/biblio/1055416>.
- [17] M. Corradini, M. Anderson, Y. Hassan, A. Tokunohiro, Experimental Studies of NNGP Reactor Cavity Cooling System With Water, <http://dx.doi.org/10.2172/1063993>, URL <https://www.osti.gov/biblio/1063993>.
- [18] R. Vaghetto, Y. Hassan, Modeling the thermal-hydraulic behavior of the reactor cavity cooling system using RELAP5-3D, *Ann. Nucl. Energy* 73 (2014) 75–83.
- [19] Q. Lv, A. Kraus, Z. Ooi, R. Hu, D. Lisowski, FY21 progress on computational modeling of the water-based NSTF, Tech. Rep. ANL-ART-235, Argonne National Laboratory, 2021.
- [20] D. Lisowski, C. Gerardi, R. Hu, D. Kilsdonk, N. Bremer, A. Kraus, M. Bucknor, S. Lomperski, M. Farmer, Water NSTF design, instrumentation, and test planning, Tech. Rep. ANL-ART-98, Argonne National Laboratory, 2017.
- [21] D. Lisowski, Q. Lv, R. Hu, A. Kraus, N. Bremer, D. Kilsdonk, M. Farmer, RCCS testing with the water-based NSTF: Year-1 single-phase results, Tech. Rep. ANL-ART-175, Argonne National Laboratory, 2019.
- [22] D. Lisowski, Q. Lv, N. Bremer, R. Hu, A. Kraus, D. Kilsdonk, S. Lomperski, M. Farmer, Report on year-2 of water NSTF matrix testing: Two-phase baseline and repeatability, Tech. Rep. ANL-ART-206, Argonne National Laboratory, 2020.
- [23] Q. Lv, M. Jasica, D. Lisowski, M. Farmer, Report on year-3 of water NSTF matrix testing: Two-phase parametric test series, Tech. Rep. ANL-ART-230, Argonne National Laboratory, 2021.
- [24] RELAP5, RELAP5-3D code manual volume IV: Models and correlations, Tech. Rep. INL/MIS-15-36723, Idaho National Laboratory, 2015.
- [25] Q. Lv, A. Kraus, R. Hu, M. Bucknor, D. Lisowski, D. Bremer, Progress report on computational analyses of water-based NSTF, Tech. Rep. ANL-ART-103, Argonne National Laboratory, 2017.
- [26] Z. Ooi, Q. Lv, R. Hu, D. Lisowski, Modeling of a Large Scale RCCS Operating at Two-Phase Transient Conditions with RELAP5-3D, 2022 ANS Winter Meeting and Technological Expo, 2022.
- [27] Z. Ooi, Q. Lv, R. Hu, M. Jasica, D. Lisowski, FY22 progress on computational modeling of the water-based NSTF, Tech. Rep. ANL-ART-257, Argonne National Laboratory, 2022, <http://dx.doi.org/10.2172/1888758>, URL <https://www.osti.gov/biblio/1888758>.
- [28] M.S. Plesset, S.A. Zwick, The growth of vapor bubbles in superheated liquids, *J. Appl. Phys.* 25 (4) (1954) 493–500.
- [29] K. Lee, D. Ryley, The evaporation of water droplets in superheated steam, *J. Heat Transfer* 90 (4) (1968) 445–451.
- [30] W. Fullmer, V. Kumar, C. Brooks, Validation of RELAP5/MOD3.3 for subcooled boiling, flashing and condensation in a vertical annulus, *Prog. Nucl. Energy* 93 (2016) 205–217.
- [31] Z. Ooi, V. Kumar, C. Brooks, Validation of the interfacial area transport equation coupled with the void transport equation for prediction of flashing flows, *Nucl. Sci. Eng.* 194 (8–9) (2020) 598–619.
- [32] Z. Ooi, C. Brooks, Two-group interfacial area transport equation coupled with void transport equation in adiabatic steam water flows, *Int. J. Heat Mass Transfer* 177 (2021) 121531.
- [33] A. Mangal, V. Jain, A. Nayak, Capability of the RELAP5 code to simulate natural circulation behavior in test facilities, *Prog. Nucl. Energy* 61 (2012) 1–16.
- [34] Q. Lv, M. Jasica, R. Hu, Z.J. Ooi, M. Farmer, D. Lisowski, FY23 report on water NSTF testing at two-phase conditions: Off-normal scenarios, Tech. Rep. ANL-ART-274, Argonne National Laboratory (ANL), Argonne, IL (United States), 2023.
- [35] M. Furuya, F. Inada, A. Yasuo, Inlet throttling effect on the boiling two-phase flow stability in a natural circulation loop with a chimney, *Heat Mass Transf.* 37 (2–3) (2001) 111–115.